



An advanced framework for tolerance analysis of cam-clamping devices integrating unified Jacobian–Torsor model, Monte Carlo simulation, and bootstrap technique

Belkacem Aoufi¹ · Hacene Ameddah¹ · Mohamed Slamani^{2,3} · Mustapha Arslane^{2,3}

Received: 13 February 2024 / Accepted: 1 August 2024 / Published online: 15 August 2024
© The Author(s), under exclusive licence to Springer-Verlag London Ltd., part of Springer Nature 2024

Abstract

Uncertainty analysis is essential for estimating variability within specified tolerances, particularly in three-dimensional (3D) assembly tolerance analysis. This study introduces a novel analytical approach for assessing assembly deviations, integrating the Jacobian–Torsor model with the bootstrap technique. The Jacobian–Torsor model combines the efficiency of representing tolerances with the adaptability of the Jacobian matrix for their propagation. This computerized method, based on the unified Jacobian–Torsor approach, focuses on cam-clamping devices, specifically the fastening flange component. The novelty of this study lies in the application of the bootstrap technique, a Monte Carlo Simulation approach, for uncertainty analysis to estimate variability within specified tolerances. A comprehensive comparison of statistical methods—bootstrap, stratified sampling, Bayesian statistics, and analytical methods—demonstrates the advantages of the Bootstrap approach. The results emphasize its user-friendliness and precision, even with complex shapes. The primary aim is to highlight the utility of the unified Jacobian–Torsor method for tolerance analysis. An experiment involving the fastening flange assembly illustrates the practical application of this approach. The findings confirm the effectiveness of the proposed method, demonstrating its accuracy and reliability for cam-clamping devices in real-world assembly scenarios with intricate geometries.

Keywords Tolerance analysis · Jacobian–Torsor model · Monte Carlo simulation · Unified Jacobian–Torsor · Mechanical assemblies · Bootstrap technique

1 Introduction

The advancement of manufacturing technologies and the increasing demand for complex and highly precise components have necessitated the development of advanced tolerance methods. These methods, based on functional approaches, allow for the consideration of interactions

between different surfaces within an assembly and accurately calculating the impact of tolerances on the performance of complex parts. This method addresses the challenges posed by modern manufacturing by enabling engineers and designers to specify more precise tolerances while ensuring product quality and functionality.

To address these challenges, 3D tolerance methods are increasingly being utilized. These methods, which combine dimensional and geometric tolerances, allow for a more precise consideration of interactions between different surfaces of a component compared to traditional methods. Tolerance is represented and transferred into three dimensions (3D) through the novel technique of three-dimensional (3D) tolerance analysis. Compared to traditional methods, the 3D method has the advantage of accounting for both dimensional and geometric tolerances [1]. Automatic tolerancing of complex shapes using the Jacobian–Torsor model is a rapidly expanding field in the industry and design domain. The benefits of the Torsor model, which excels in representing tolerances, are seamlessly merged with those of the

✉ Mohamed Slamani
mohamed.slamani@univ-msila.dz

¹ Laboratory of Innovation in Construction, Eco-Design, and Seismic Engineering (LICEGS), Faculty of Technology, Department of Mechanical Engineering, University of Batna 2, 0500 Batna, Algeria

² MMS Lab, Faculty of Technology, University of M'sila, University Pole, Road Bourdj Bou Arreiridj, M'sila 28000, Algeria

³ Mechanical Engineering Department, Faculty of Technology, University of M'sila, University Pole, Road Bourdj Bou Arreiridj, M'sila 28000, Algeria

Jacobian matrix, specifically designed for tolerance propagation, within the unified Jacobian–Torsor model [2, 3].

Automatic tolerancing of intricate shapes involves the automated assessment and specification of dimensional and geometric tolerances for complex-shaped components. Traditionally, manually tolerancing such complex shapes has been a challenging and subjectively interpreted task, leading to errors and substantial time consumption. However, the unified model plays a crucial role in the computer-aided tolerance field by integrating the strengths of both Jacobian and small displacement torsor (SDT) methods [4]. This model excels in representing and propagating complex geometric variations with high precision [5, 6]. It takes into account the kinematic relationships among different features of a part, enabling a thorough evaluation of the effects of geometric variations on the assembly and the overall performance of the final product.

By using the Jacobian–Torsor model, it becomes possible to automatically generate tolerance specifications for complex shapes, taking into account assembly constraints, functional interactions, and manufacturing requirements. This reduces errors, optimizes design and manufacturing processes, and ensures compliance with quality requirements. This approach offers numerous benefits, including reduced production costs, improved efficiency and accuracy, and increased product reliability. Enabling the automatic tolerancing of complex shapes, the Jacobian–Torsor model opens up new possibilities for advanced design, high-precision manufacturing, and meeting customer requirements in the industry.

Over the past three decades, extensive fundamental research has delved into the mathematical foundations of tolerance analysis. Among the various models and concepts employed for tolerance representation, variational geometry stands out as a prominent approach [7, 8]. Additional methodologies include the vector approach [9] tolerance map (T-Map) [10], topologically and technologically related surfaces (TTRS) [11], degrees of freedom (DOF) [12, 13], variational class [14, 15], small displacement torsor (SDT) [16, 17], matrix [18], and other techniques like the linearization method for tolerance propagation, network of zones and references [19], Taguchi method [20], state space [21], Jacobian matrix [22, 23], and variational method [24].

Over the years, many models have been created to represent and propagate 3D tolerance. Fleming [19], employs a network of arc-connected zones and references, on which constraints are positioned to show geometric relationships. To simulate tolerance propagation, Portman et Weill [25], introduce a spatially dimensioned chain in which each individual error is represented by an infinitesimal matrix. Rivest et al. [26], provide a kinematic explanation based on the characteristics of an element that is acceptable in relation to the data.

For a target entity, every possible combination of size, position, shape, and orientation is represented by the T-Map [10]. Six small displacement vectors are used in an SDT model introduced by Clément et al. [23]. Laperrière and Lafond [27], describe tolerance using virtual joints and propagate tolerance using a Jacobian matrix. The benefits of the Torsor model and the Jacobian matrix are combined in the unified Jacobian–Torsor model proposed by Desrochers et al. [2]. Thanks to computer-aided tolerance (CAT), some of the aforementioned models have been widely used.

Yi et al. [28] present an advanced 3D assembly tolerance analysis method for digital twin precision analysis, addressing limitations of current approaches that miss geometric tolerances and form errors and fail to account for parallel connections. Their novel method integrates the unified Jacobian–Torsor model with skin model shapes for effective tolerance propagation and geometric representation. An improved approach calculates positioning errors in serial and parallel connections using progressive contact and algebraic methods. The method's statistical calculation scheme is validated through a case study, showcasing its effectiveness.

Peng and Peng [29] present an iterative statistical tolerance design method to guide economical and effective tolerance selection. They derive a unified Jacobian–Torsor model from assembly functional requirements (FR) and functional elements (FEs). Monte Carlo simulations generate variations within tolerance zones, and statistical analysis of these simulations determines FR limits. Critical FE tolerances are adjusted iteratively until the calculated FR aligns with the imposed FR. A case study demonstrates the method's cost-effectiveness and precision relaxation compared to traditional deterministic tolerancing.

Roth et al. [30] explore the integration of sampling-based tolerance analysis into tolerance-cost optimization, emphasizing its industrial significance for cost-effective tolerance allocation. They address the problem of sampling-induced variance, which impacts the stability, reproducibility, and reliability of the optimization process. The article proposes methods to mitigate and manage these uncertainties, improving the reliability of the optimization. Their recommendations offer guidance for researchers and practitioners to achieve consistent and dependable tolerance-cost optimization outcomes.

Ding et al. [31] address challenges in aero-engine rotor assembly, focusing on the impact of manufacturing errors and assembly variations on engine reliability. They address issues in three-dimensional variation analysis, specifically over-positioning of multiple datums and variation propagation in rotating components. They developed an improved Jacobian–Torsor model, enhancing rotation regulation and feature interaction. Their multi-stage optimization of a four-stage aero-engine rotor assembly demonstrates the model's

effectiveness in precision prediction and analysis during the design phase.

Liu et al. [32] introduce a new method for assembly tolerance analysis by combining the Jacobian model with the skin model shape. This technique models small displacements and uses point cloud representations to simulate actual toleranced surfaces. It effectively manages geometric tolerances throughout the product lifecycle, allowing accurate analysis of kinematic variations and functional requirements. While still under development, this method supports design, manufacturing, and inspection by quantitatively analyzing the impact of multiple tolerances on key characteristics. The innovative integration of these models provides a comprehensive approach to geometric tolerance consideration in assembly processes.

To improve the machining performance of complex shapes, Wong et al. [33] proposed a new solution for precision machining of thin-walled turbine blades. The integrated analysis method combines geometric tolerance localization analysis and structural deformation prediction based on the finite element method (FEM). Zhang et al. [34] employed an analytical methodology for tolerance analysis and synthesis in a cam and translation follower system. They distributed tolerance values associated with design requirements in terms of functionality or output precision among identified design tolerances using a sequential quadratic programming (SQP) algorithm. Chang et al. [30] stress the significance of tolerance analysis in the development and production of cam mechanisms, and the necessity of computer calculations and mathematical modelling to ascertain the optimal tolerance values.

Cam-clamping devices are extensively utilized in diverse machining fixtures due to their capacity for swift action, generation of substantial clamping force, and execution of specified functions, paths, and motions. These capabilities surpass those of pure linkages when evaluated through the lens of kinematic design. However, the irregular shape of cams [35–37] presents a greater challenge in terms of accurate machining compared to the more straightforward dimensions of linkages. Even minor deviations in the cam contour within machining fixtures can result in excessive noise, wear, and vibrations [36–38], which adversely affect the precision and reproducibility of machined components.

To achieve kinematic accuracy and dynamic performance at an acceptable level, the manufacturing and assembly errors in a cam-clamping device must stay within specified tolerances. Consequently, the processes of tolerance analysis and synthesis [39–41] become pivotal in the design and production of precise cam-clamping devices. Tolerance analysis assesses output motion errors resulting from known deviations or specified tolerances in the design parameters, while tolerance synthesis focuses on identifying the optimal

combination of tolerances, considering restricted output motion errors and controlled production costs.

In the context of design for manufacturing and assembly (DFMA) [42, 43], it is essential to specify the largest (or optimal) values for the cam profile and the tolerance of each design parameter. This is crucial for simplifying the fabrication of components in a cam-clamping device. Additionally, the optimal combination of tolerances must align with the operational or functional requirements of the output motion. Therefore, the development of mathematical tools for both tolerance analysis and synthesis is imperative to facilitate the production of precise cam-clamping devices.

This paper aims to develop a computerized method based on the unified Jacobian–Torsor approach to conduct tolerance analysis on cam-clamping devices, particularly those with complex surfaces such as fastening flanges. The innovation lies in applying the Unified Jacobian–Torsor method to assess tolerance among functional components, including irregularly shaped mechanical parts, within a cam-clamping device. This method offers a more precise and integrated approach for evaluating the quality and dimensional variations within the assembly.

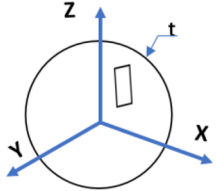
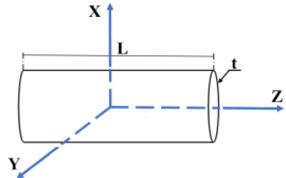
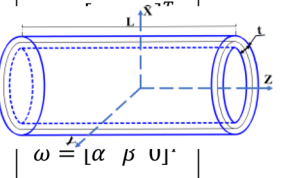
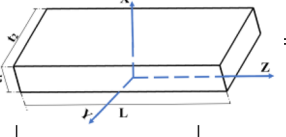
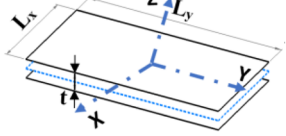
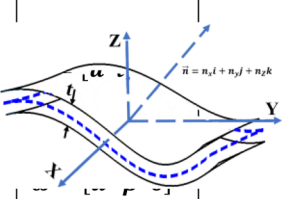
Additionally, the paper introduces the innovative application of the bootstrap technique for uncertainty analysis, enhancing the robustness of the tolerance assessment. The bootstrap technique, a Monte Carlo simulation approach, is leveraged to estimate the uncertainty associated with the analytical results, providing valuable insights into potential variability within specified tolerances. This dual integration of the unified Jacobian–Torsor method and the bootstrap technique contributes to a more comprehensive and advanced methodology for precision engineering in cam-clamping devices.

2 Small displacement torsor (SDT)

A variety of geometric shapes, such as parallel planes or surfaces, parallelepiped faces, coaxial cylinders, and cylindrical faces, are frequently used to represent a three-dimensional tolerance zone. Table 1 provides these 3D tolerance zones coupled with the Small Degrees of Freedom (SDOF) vectors that correspond to them, along with a general description of the elements of these SDOF vectors in modal interval expressions [44].

The modeling of these 3D tolerance zones greatly benefits from the use of small displacement torsor (SDT) parameters. The six parametric intervals of the SDT are particularly well-suited to this task, as they allow for representing all potential variations in terms of size, shape, orientation, position, and out-of-roundness of a geometric element relative to its nominal position within the tolerance zone. This approach provides essential precision and flexibility to comprehensively describe geometric variations in a three-dimensional context, which is crucial for

Table 1 Modal interval description of 3D tolerance zones in SDOF vector form [44]

3D tolerance zone	SDDF vectors description	
Spherical zone 	$u = \left[-\frac{t}{2}, \frac{t}{2}\right], v = \left[-\frac{t}{2}, \frac{t}{2}\right]$ $w = \left[-\frac{t}{2}, \frac{t}{2}\right]$ $u^2 + v^2 + w^2 = \left[0, \left(\frac{t}{2}\right)^2\right]$	
Cylindrical zone 	$u = \left[-\frac{t}{2}, \frac{t}{2}\right], v = \left[-\frac{t}{2}, \frac{t}{2}\right]$ $\alpha = \left[-\frac{t}{L}, \frac{t}{L}\right], \beta = \left[-\frac{t}{L}, \frac{t}{L}\right]$ $\left(u + \frac{\alpha L}{2}\right)^2, \left(v + \frac{\beta L}{2}\right)^2 = \left[0, \left(\frac{t}{2}\right)^2\right]$	
Two coaxial Cylindrical 	$u = \left[-\frac{t}{2}, \frac{t}{2}\right], v = \left[-\frac{t}{2}, \frac{t}{2}\right]$ $\alpha = \left[-\frac{t}{L}, \frac{t}{L}\right], \beta = \left[-\frac{t}{L}, \frac{t}{L}\right]$ $\left(u + \frac{\alpha L}{2}\right)^2, \left(v + \frac{\beta L}{2}\right)^2 = \left[0, \left(\frac{t}{2}\right)^2\right]$	$\omega = [\alpha \ \beta \ 0]^T$
Parallelepiped zone 	$u = \left[-\frac{t}{2}, \frac{t}{2}\right], v = \left[-\frac{t}{2}, \frac{t}{2}\right]$ $\alpha = \left[-\frac{t}{L_x}, \frac{t}{L_x}\right], \beta = \left[-\frac{t}{L_y}, \frac{t}{L_y}\right]$ $ u + \left \frac{\alpha L_x}{2}\right = \left[0, \frac{t_1}{2}\right], v + \left \frac{\beta L_y}{2}\right = \left[0, \frac{t_2}{2}\right]$	$\omega = [\alpha \ \beta \ 0]^T$
Two parallels plans 	$w = \left[-\frac{t}{2}, \frac{t}{2}\right]$ $\alpha = \left[-\frac{t}{L_y}, \frac{t}{L_y}\right], \beta = \left[-\frac{t}{L_x}, \frac{t}{L_x}\right]$ $ w + \left \frac{\alpha \cdot L_y}{2}\right + \left \frac{\beta \cdot L_x}{2}\right = \left[0, \frac{t}{2}\right]$	
Two parallel Surfaces 	$u = \left[-\frac{t}{2} \cdot n_x, \frac{t}{2} \cdot n_x\right]$ $v = \left[-\frac{t}{2} \cdot n_y, \frac{t}{2} \cdot n_y\right]$ $w = \left[-\frac{t}{2} \cdot n_z, \frac{t}{2} \cdot n_z\right]$ $\alpha = \left[-\frac{t}{l_{yz}}, \frac{t}{l_{yz}}\right], \beta = \left[-\frac{t}{l_{xz}}, \frac{t}{l_{xz}}\right]$ $\gamma = \left[-\frac{t}{l_{xy}}, \frac{t}{l_{xy}}\right]$ $f(x) = (u, v, w, \alpha, \beta, \gamma) = 0$	

ensuring compliance of parts and assemblies in applications requiring strict tolerances. A detailed inventory of the various standard tolerance zones, together with torsor representations and related geometric restrictions, was compiled by Desrochers et al. [2]. Several typical tolerance zone examples are included in Table 1, along with

information on their forms, related torsor matrices, and underlying geometric restrictions. Each geometric limitation constrains the range of variation of the different torsor components, as illustrated in Table 2. Following their incorporation into the torsor matrices, these geometric restrictions can be expressed as follows (Eq. (1)):

Table 2 Zones of tolerance and related torsor parameters [2]

Tolerance zones	Zone shapes	Torsor matrixes	Constraints
Space with in a cylinder		$\begin{bmatrix} \alpha & u \\ \beta & v \\ 0 & 0 \end{bmatrix}$	$u = \left[-\frac{t}{2}, \frac{t}{2}\right], v = \left[-\frac{t}{2}, \frac{t}{2}\right],$ $\alpha = \left[-\frac{t}{L}, \frac{t}{L}\right], \beta = \left[-\frac{t}{L}, \frac{t}{L}\right]$ $u^2 + v^2 \leq \frac{t^2}{4}$
Space between two coaxial cylinders		$\begin{bmatrix} \alpha & u \\ \beta & v \\ 0 & 0 \end{bmatrix}$	$\alpha = \left[-\frac{t}{L}, \frac{t}{L}\right], \beta = \left[-\frac{t}{L}, \frac{t}{L}\right]$ $u = \left(\frac{t}{2}\right) \cos \theta$ $v = \left(\frac{t}{2}\right) \sin \theta$ $u^2 + v^2 \leq \frac{t^2}{4}$
Space with in a parallelepiped		$\begin{bmatrix} \alpha & u \\ \beta & v \\ 0 & 0 \end{bmatrix}$	$u = \left[-\frac{t_2}{2}, \frac{t_2}{2}\right]$ $v = \left[-\frac{t_1}{2}, \frac{t_1}{2}\right]$ $\alpha = \left[-\frac{t_1}{L}, \frac{t_1}{L}\right]$ $\beta = \left[-\frac{t_2}{L}, \frac{t_2}{L}\right]$
Space between two parallel planes		$\begin{bmatrix} \alpha & u \\ \beta & v \\ \gamma & w \end{bmatrix}$	$w = \left[-\frac{t_2}{2}, \frac{t_2}{2}\right]$ $\alpha = \left[-\frac{t_1}{L_2}, \frac{t_1}{L_2}\right]$ $\beta = \left[-\frac{t_2}{L_1}, \frac{t_2}{L_1}\right]$
Space between two equidistant surfaces		$\begin{bmatrix} \alpha & u \\ \beta & v \\ \gamma & w \end{bmatrix}$	Undefined

$$T = \{\rho\epsilon\} = \left\{ \begin{array}{l} \left[\begin{array}{l} \alpha, \bar{\alpha} \\ \beta, \bar{\beta} \\ \gamma, \bar{\gamma} \end{array} \right] \\ \left[\begin{array}{l} u, \bar{u} \\ v, \bar{v} \\ w, \bar{w} \end{array} \right] \end{array} \right\} \quad (1)$$

3 Integration of the Jacobian–Torsor model

The integration of the Jacobian–Torsor model highlights the fundamental concepts and tools of the proposed unified model for cam clamping devices in scenarios involving

the assembly of complex geometries. This integration involves the visualization of Functional Elements (FEs), which represent the structure of a mechanical system through a contact graph, categorizing these elements into real and fictitious components. Pairs of Contact Functional Elements (PCFE) are established when there is physical contact between two functional elements, symbolically represented by (C). Additionally, Pairs of Internal Functional Elements (PIFE) are formed when two FEs on the same part come into contact, symbolized by (I). Functional requirements (FR) define the relationships between FEs located on separate parts, particularly focusing on the space between end surfaces, depicted by double-oriented arrows. The complete set of these desired functional requirements is designated as (FR).

4 Unified Jacobian–Torsor model

To create the unified Jacobian–Torsor model, the benefits of both approaches are combined: the Torsor model is helpful in characterizing tolerances, and the Jacobian matrix is used to propagate tolerances. Jacobian matrices describe the locations and relative orientations between local frames and the global frame of reference. This combination allows complex geometric changes in this model to be accurately represented and transmitted. The model considers the kinematic links among various mechanism aspects, allowing for the evaluation of the effects of geometric alterations on product performance and assembly. The final statement of a unified Jacobian–Torsor model can be written as follows: [2, 3]:

$$[FR] = [J] \cdot [FE_S] \tag{2}$$

$$\begin{bmatrix} [\underline{u}, \bar{u}] \\ \vdots \\ [\underline{\gamma}, \bar{\gamma}] \\ \vdots \\ [-] \end{bmatrix}_{FR} = [J_1 \dots J_n] \begin{bmatrix} [\underline{u}, \bar{u}] \\ \vdots \\ [\underline{\gamma}, \bar{\gamma}] \\ \vdots \\ [-] \end{bmatrix}_{FEi} \tag{3}$$

Equations (2) and (3) allow us to understand and quantify how geometric variations propagate through the different components of an assembly, providing a powerful tool for product quality analysis and improvement.

Here, $[FR]$ represents the translational matrix $[u \ v \ w]^T$ and the rotational matrix $[\alpha \ \beta \ \gamma]^T$ in the global reference system. In this global system, $u, v,$ and w correspond to three translation vectors, while $\alpha, \beta,$ and γ represent three rotation vectors around the $x, y,$ and z axes, respectively, in the local reference systems.

On the other hand, $[FE_S]$ represents the translation and rotation matrix of the i th $[FE_i]$ in the local reference system. Finally, $[J]$ symbolizes the 6×6 Jacobian matrix for the i th pair of assembly features, with i ranging from 1 to N . The subsequent formulation can be used to express it precisely:

$$[J_1 \dots J_6]_{FEi} = \begin{bmatrix} [R_0^i]_{3 \times 3} \cdot [R_{PTi}]_{3 \times 3} \vdots [W_i^n]_{3 \times 3} \cdot [R_0^i]_{3 \times 3} \cdot [R_{PTi}]_{3 \times 3} \\ \dots \vdots \dots \vdots \\ [0]_{3 \times 3} \vdots [R_0^i]_{3 \times 3} \cdot [R_{PTi}]_{3 \times 3} \end{bmatrix}_{6 \times 6} \tag{4}$$

The relationship between the minor variation of all functional components $[FE]$ and the intended functional requirement $[FR]$ is expressed using the Jacobian matrix. The matrix’s columns are derived from different homogeneous transformation matrices that connect the functional elements’ $[FE]$ and functional requirements’ $[FR]$ reference frames [45].

The geometric relationships between the 0th and i th consecutive references are defined by the transformation matrices $[T_0^i]$. More precisely, a rotation matrix and a translation vector can be extracted from each transformation matrix

[46]. Therefore, the following representation can be used to represent a transformation matrix:

$$[T_0^i] = \begin{bmatrix} [R_0^i]_{3 \times 3} & \dots & [P_0^i]_{3 \times 1} \\ \vdots & \ddots & \vdots \\ [0] & \dots & [1] \end{bmatrix} = \begin{bmatrix} \bar{C}_{1i} & \bar{C}_{2i} & \bar{C}_{3i} & \bar{d}_i \\ 0 & 0 & 0 & 1 \end{bmatrix}_{4 \times 4} \tag{5}$$

where $[R_0^i]_{3 \times 3}$ represents the orientation transformation matrix of the i th FE_S relative to the global reference system (designated as the 0th frame). This matrix is defined in Eq. (6).

$[R_{PTi}]_{3 \times 3}$ is a projection matrix, indicating the projection coefficient of the three axes in the i th local reference system, depending on the direction of variation of the tolerance zone. The product $[R_0^i]_{3 \times 3} \cdot [R_{PTi}]_{3 \times 3}$ in Eq. (4), ensures that the Jacobian matrix takes into account the inclination of the reference system of a projected tolerance zone.

$$[R_0^i]_{3 \times 3} = [\bar{C}_{1i} \ \bar{C}_{2i} \ \bar{C}_{3i}] \tag{6}$$

The vectors within the matrix $[R_0^i]_{3 \times 3}$ illustrate the orientation of i th local reference system concerning the global reference system 0th frame. The columns $\bar{C}_{1i}, \bar{C}_{2i},$ and \bar{C}_{3i} correspond to the unit vectors along the axes $x_i, y_i,$ and z_i of reference mark i th within reference global 0th. The position vector, denoted as $d_i = [dx_i \ dy_i \ dz_i]$, indicates the location of the origin of reference frame i th with respect to reference mark 0th.

$[W_i^n]_{3 \times 3}$ represents the position transformation matrix between the i th and n th local reference system, which is anti-symmetric. To express it, use the formula below.

$$[W_i^n]_{3 \times 3} = \begin{bmatrix} 0 & -dz_i^n & dy_i^n \\ dz_i^n & 0 & -dx_i^n \\ -dy_i^n & dx_i^n & 0 \end{bmatrix} \tag{7}$$

In the i th and n th local reference systems with respect to the global reference system, the coordinate values around the $x, y,$ and z axes are represented by the variable $dx_i^n = dx_n - dx_p, dy_i^n = dy_n - dy_p,$ and $dz_i^n = dz_n - dz_p; dx_i, etdx_i^n, dy_i, etdy_i^n,$ and dz_i and $ddz_i^n,$ respectively. The constraint relationship between surface entities and the tolerance variation domain interval will be determined by the surface type and tolerance value of FE_S . In the tolerance zone where $[FE_i]$ must be located, every parameter of $[FE_S]$ will be restricted to the allowable range of the variation domain. Thus, the conventional unified Jacobian–Torsor model can be described as follows by applying the principle of addressing variances and constraints imposed by surface features in mechanical assemblies. The Jacobian matrices for internal and kinematic pairs are computed using the unified Jacobian–Torsor model, and they are crucial for building the final expression of the unified model.

$$\begin{bmatrix} \underline{u}, \bar{u} \\ \underline{v}, \bar{v} \\ \underline{w}, \bar{w} \\ \underline{\alpha}, \bar{\alpha} \\ \underline{\beta}, \bar{\beta} \\ \underline{\gamma}, \bar{\gamma} \end{bmatrix}_{FR} = \left[[J_1 J_2 J_3 J_4 J_5 J_6]_{EF1} \dots [J_1 J_2 J_3 J_4 J_5 J_6]_{EFN} \right] \begin{bmatrix} \underline{u}, \bar{u} \\ \underline{v}, \bar{v} \\ \underline{w}, \bar{w} \\ \underline{\alpha}, \bar{\alpha} \\ \underline{\beta}, \bar{\beta} \\ \underline{\gamma}, \bar{\gamma} \end{bmatrix}_{FE1} \dots \begin{bmatrix} \underline{u}, \bar{u} \\ \underline{v}, \bar{v} \\ \underline{w}, \bar{w} \\ \underline{\alpha}, \bar{\alpha} \\ \underline{\beta}, \bar{\beta} \\ \underline{\gamma}, \bar{\gamma} \end{bmatrix}_{FEN} \quad (8)$$

Each matrix represents contributions to the functional requirements (FR).

N: Number of wrenches in a chain.

(*u, v, …, γ*): Minimum limits of *u, v, …, γ*

(*ū, v̄, …, γ̄*): Maximum limits of *u, v, …, γ*

The interval matrix representation, as proposed, better represents reality in tolerancing.

The dispersions of a functional requirements (FR) are represented by the column matrix [FR]. The column matrix *FE_S* contains the dispersions of functional elements and uncertainties of a contact pair. Both column matrices contain tolerance intervals in translation and rotation. This expression allows presenting tolerancing with tolerance zones instead of points. Indeed, some values of *u, v, …, γ* contain zero values. To make calculations easier, some of the primary wrench model vectors in Table 2 can be set to zero in accordance with Hervé's displacement set theory [47].

5 Unified Jacobian–Torsor tolerance model organization

The methodology for analyzing tolerances involves five key steps. First, it entails establishing the sequence of events relevant to the functional requirement or system under examination. The second step involves deriving the torsors of internal functional elements, which define their degrees of freedom, permissible small movements, and constraints. Subsequently, obtaining the contact zone torsors constitutes the third step. The fourth step employs Jacobian matrices to represent the relative positions and orientations of the torsors within the chosen kinematic chain. Finally, the torsor and Jacobian are integrated to form a matrix equation, the solution of which yields the limits of the functional requirements (FR) being analyzed. Figure 1 illustrates the organizational structure of these five steps in the unified J-T model.

6 Three-dimensional dimension chain

As mentioned earlier, the proposed approach was applied on a cam-clamping device. The cam-clamping device comprises two essential elements: firstly, the fixed part represented by a flange, serving as the assembly's foundation, and secondly, the movable part consisting of an irregular-shaped component known as a cam. This movable piece is critical to the fastening mechanism and plays an essential role in the overall functionality of the assembly.

To achieve the utilization of a unified model, it is crucial to follow a series of important preliminary steps to precisely define the dimensional specifications related to the functional requirements (FR) of the mechanism. The model relies on identifying contact surfaces between the various components of the mechanism. This identification of surfaces is essential for constructing the linkage diagram of the mechanism in question. To illustrate these concepts, refer to Fig. 2, which represents an assembly consisting of two parts, one inserted into the other. This figure also relies on the functional requirements (FR), which expresses a requirement related to the operation or assembly of the two parts, in order to visually represent the various terms involved.

The cam-clamping device, consisting of two different parts—1: a fixed part composed of a flange, and 2: a movable part consisting of a complex piece (a cam)—is represented in Fig. 2 to illustrate the application of the proposed tolerance analysis method. The functional requirement (FR) represents the variation in the circular clearance between the two circular surfaces of the movable part (part 2) and the fixed part (part 1) to achieve optimal working performance.

Particulars of the mechanical drawing and critical dimensional specifications of the cam-clamping device are presented in Fig. 3. A dimensional connection graph is constructed around the FR of this assembly after the required local coordinate frames have been defined and the effective feature surfaces associated with the tolerance analysis have been determined. The effective feature surfaces between the two parts are identified once all effective geometric features have been identified and local coordinate frames have been defined. This allows for the ascertainment of variations in circular displacement between the two circular surfaces, as illustrated in Fig. 4. By locating these surfaces, the linkage diagram of the associated mechanism can be created, and as Fig. 5 illustrates, a connection graph of the restraining flange mechanism can be built.

Figures 4 and 5 illustrate six impactful geometric features associated with the functional requirement (FR) of this assembly. These features include *FE₀*, representing the arbitrary shape in relation to the two slots (1–2) of the fixed flange. *FE₁* and *FE₂* form an internal pair signifying

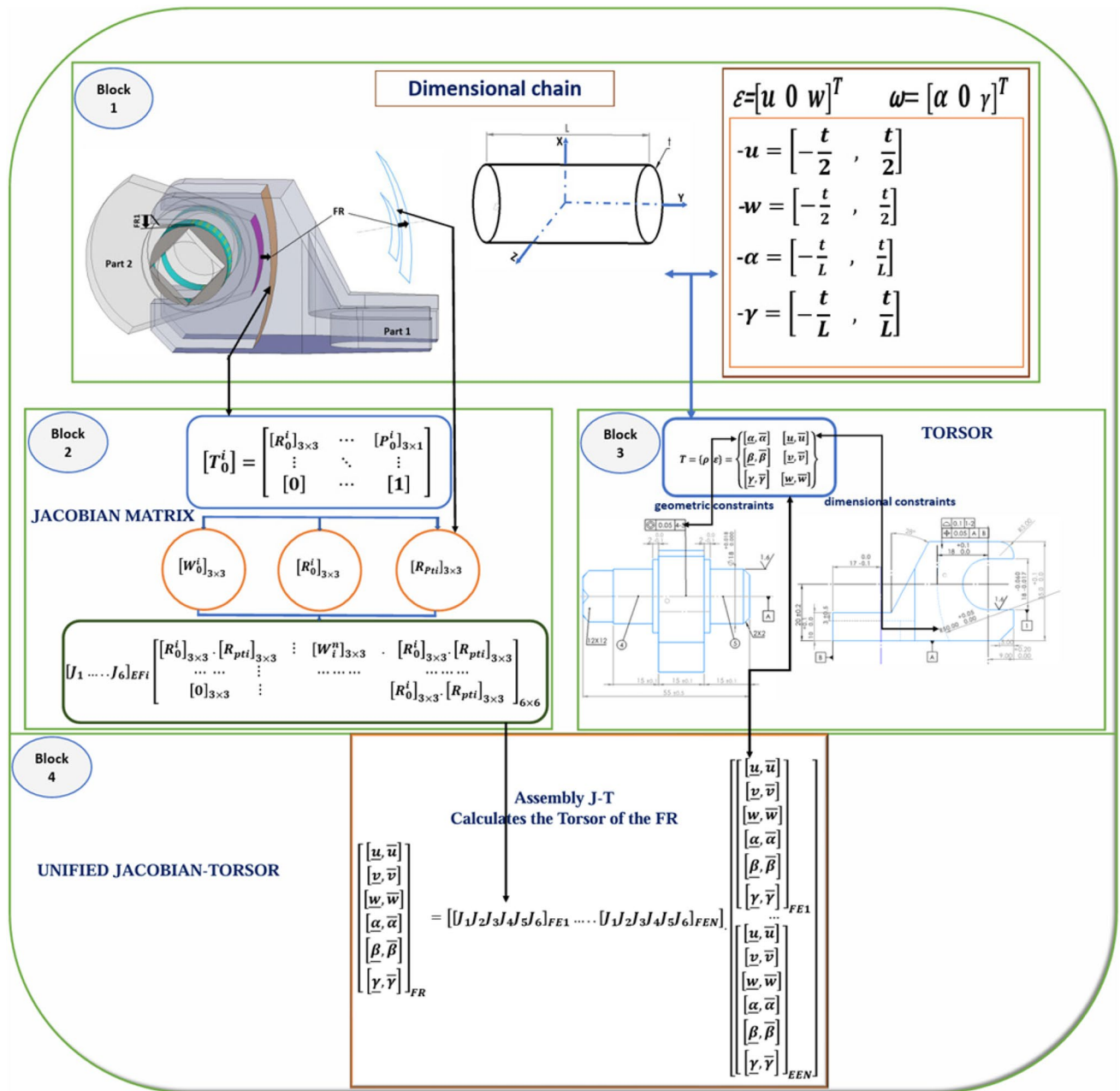


Fig. 1 The five key steps of organizational structure in the unified model (J-T)

coaxiality relative to the two slots (1–2), collectively referred to as FE_{slo} . FE_3 characterizes the arbitrary shape of the cam concerning the two axes (4–5). $FR1$ denotes the operational clearance between the two slots (1–2) and the two axes (4–5) of the cam. FE_4 and FE_5 , functioning as an internal pair, denote coaxiality concerning the two axes (4–5) of the cam, grouped into a single functional element known as FE_{axe} . Lastly, FE_6 represents the distance between the axis of the outer radius R20 and the two axes (4–5) of the cam, respectively.

The resulting kinematic chain contains five internal pairs (FE_0, FE_{slo}), (FE_1, FE_2) belonging to the fixed part, (FE_3, FE_{axe}), (FE_4, FE_5), and (FE_6, FE_{axe}) belonging to the movable part, as well as a contact pair (FE_{slo}, FE_{axe}).

Note that there are two functional requirements (FR and $FR1$). FR represents the functional clearance under study, while $FR1$ applies between (FE_{axe}, FE_{slo}) and is defined by the functional fit H7/g6 of the bore $18_{0,00}^{+0,018}$ of the fixed flange housing and the diameter $18_{-0,017}^{-0,06}$ of the camshafts.

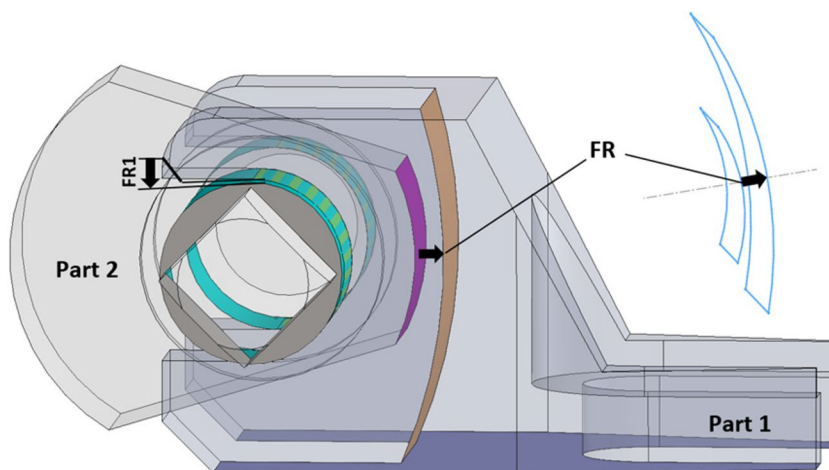
We assumed that the longitudinal plane and the reference points were situated in the middle of the tolerance zone.

Six torsors are connected in series to form the cumulative torsor $T_{3/0}$, which represents the torsor of the difference between features FE_0 and FE_3 . These torsors are $T_{slo/0}$, $T_{axe/3}$, $T_{2/1}$, $T_{axe/slo}$, $T_{4/5}$, $T_{6/axe}$. Next, a direction of analysis specified along the modest translation displacement normal to surfaces 0 and 3 of the functional requirements (FR) under study must be projected onto these six torsors. From each transformation matrix, a rotation matrix and a translation vector can be constructed, as indicated in Eq. (5). Additionally, all surfaces are positioned vertically inside

the mechanism, which means that their orientation corresponds to that of the tolerance zone. Under these conditions, all $[R_{PTi}]_{3 \times 3}$ projection matrices are linked to identity matrices so that the tolerance zones respect the movement. The mathematical specifics for the clamping mechanism's traditional torsors, also known as intermediate torsors, are provided in Table 2. Equation (9) comprises six Jacobian matrices that describe the geometric and dimensional relationships between the assembly pairs FR and FE. These matrices can be expressed as follows:

$$FR = \begin{bmatrix} \begin{bmatrix} 1 & 0 & 0 & 0 & 0 \\ 0 & 1 & 0 & 0 & 0 \\ 0 & 0 & 1 & 0 & 0 \\ 0 & 0 & 0 & 1 & 0 \\ 0 & 0 & 0 & 0 & 1 \end{bmatrix}_{FE_1} & \begin{bmatrix} 1 & 0 & 0 & 0 & 0 \\ 0 & 1 & 0 & 0 & 3 \\ 0 & 0 & 1 & 0 & -3 \\ 0 & 0 & 0 & 1 & 0 \\ 0 & 0 & 0 & 0 & 1 \end{bmatrix}_{FE_4} \\ \begin{bmatrix} 1 & 0 & 0 & 0 & 0 \\ 0 & 1 & 0 & 0 & 18 \\ 0 & 0 & 1 & 0 & -18 \\ 0 & 0 & 0 & 1 & 0 \\ 0 & 0 & 0 & 0 & 1 \end{bmatrix}_{FE_2} & \begin{bmatrix} 1 & 0 & 0 & 0 & 0 \\ 0 & 1 & 0 & 0 & 18 \\ 0 & 0 & 1 & 0 & -18 \\ 0 & 0 & 0 & 1 & 0 \\ 0 & 0 & 0 & 0 & 1 \end{bmatrix}_{FE_5} \\ \begin{bmatrix} 1 & 0 & 0 & 0 & 0 \\ 0 & 1 & 0 & 0 & 18 \\ 0 & 0 & 1 & 0 & -18 \\ 0 & 0 & 0 & 1 & 0 \\ 0 & 0 & 0 & 0 & 1 \end{bmatrix}_{FE_3} & \begin{bmatrix} 1 & 0 & 0 & 0 & 0 \\ 0 & 1 & 0 & 0 & -23 \\ 0 & 0 & 1 & 0 & 23 \\ 0 & 0 & 0 & 1 & 0 \\ 0 & 0 & 0 & 0 & 1 \end{bmatrix}_{FE_6} \end{bmatrix} \cdot \begin{bmatrix} \begin{bmatrix} [-0.00, 0.05] \\ [0, 0] \\ [-0.00, 0.05] \\ [-0.0026, 0.0026] \\ [0, 0] \\ [-0.0026, 0.0026] \end{bmatrix}_{FE_1} \\ \begin{bmatrix} [-0.00, 0.05] \\ [0, 0] \\ [-0.00, 0.05] \\ [-0.0033, +0.0033] \\ [0, 0] \\ [-0.0033, +0.0033] \end{bmatrix}_{FE_2} \\ \begin{bmatrix} [0.000, 0.018] \\ [0, 0] \\ [0.000, 0.018] \\ [-0.00127, +0.00127] \\ [0, 0] \\ [-0.00127, +0.00127] \end{bmatrix}_{FE_3} \\ \begin{bmatrix} [0.0175, 0.0175] \\ [0, 0] \\ [-0.0175, +0.0175] \\ [-0.00175, +0.00175] \\ [0, 0] \\ [-0.00175, +0.00175] \end{bmatrix}_{FE_4} \\ \begin{bmatrix} [-0.017, -0.006] \\ [0, 0] \\ [-0.017, -0.006] \\ [-0.0009, +0.0009] \\ [0, 0] \\ [-0.0009, +0.0009] \end{bmatrix}_{FE_5} \\ \begin{bmatrix} [-0.05, +0.05] \\ [0, 0] \\ [-0.05, +0.05] \\ [-0.0066, +0.0066] \\ [0, 0] \\ [-0.0066, +0.0066] \end{bmatrix}_{FE_6} \end{bmatrix} \tag{9}$$

Fig. 2 Detailed assembly for a flange mechanism with two FRs



In Eq. (9), the inherent drawback of the presented approach is evident—assigning a unique value to each Functional Element (FE) restricts the ability to define uncertainty. In the domain of uncertainty analysis, a critical requirement is to delineate the limits surrounding the average value, providing insights into the potential range of the true value and the associated confidence level. This necessity has led to the recognition of three fundamental approaches for uncertainty evaluation on an international scale: the GUM Method, Monte Carlo simulation, and the Bayesian method. Despite its popularity, the GUM Method, also known as the classical method, relies on simplistic assumptions in its foundational formulation and exhibits limitations when applied to advanced measurement techniques [48–50].

This study employs the bootstrap technique, a Monte Carlo simulation method utilizing available data to estimate statistic or estimator uncertainty, chosen for its versatile features. A notable advantage is its capacity to bypass the need for knowledge about the true distribution, making it particularly suitable for scenarios with unknown or complex distributions.

One of the most well-known applications of the bootstrap technique involves estimating the population mean, denoted as μ , from a dataset obtained by random sampling from that population's distribution function F [51].

$$\mu = \int x dF(x) \quad (10)$$

The sample mean is a function of the empirical distribution function, namely,

$$\hat{F}(x) = \frac{1}{n} \sum_{i=1}^n I(X_i \leq x) \quad (11)$$

where X_1, X_2, \dots, X_n denote the data. Hence, the bootstrap estimator for the population mean, denoted by μ , is the sample mean \bar{X} ,

$$\bar{X} = \int x d\hat{F}(x) = \frac{1}{n} \sum_{i=1}^n X_i \quad (12)$$

Similarly, the bootstrap estimator for a population variance is the sample variance.

The developed process of integrating the bootstrap technique into statistical tolerance redesign, alongside the unified Jacobian–Torsor model, comprises the following steps:

1. Input specified assembly requirements and assign initial tolerance values for each functional element based on engineering expertise and historical knowledge.
2. Develop the expression for the Jacobian–Torsor model, defining small displacement torsor (SDT) matrices and corresponding Jacobian matrices.
3. Generate authentic random values for each SDT component, adhering to constraints, designated distributions, and a defined rejection rate. By extracting the limits of each parameter, random values are generated, leveraging the normal distribution assumption for all SDT components. The use of the Randn function in Matlab software facilitates the generation of $N=1000$ values. Subsequently, the average and standard deviation of these values are calculated.
4. The calculated mean of the data is subjected to the bootstrap process 10,000 times. This involves resampling the data with replacement 10,000 times and computing the mean during each iteration. For every iteration, 10,000 samples are randomly chosen, the mean is computed, and the process is repeated to obtain 10,000 means. These means are then used to establish the confidence interval (CI). The choice of CI type, while not heavily impactful due to the central limit theorem, typically leans towards the percentile method, recommended for its independence from the shape of the distribution. The bootstrap process is summarized in Fig. 6.

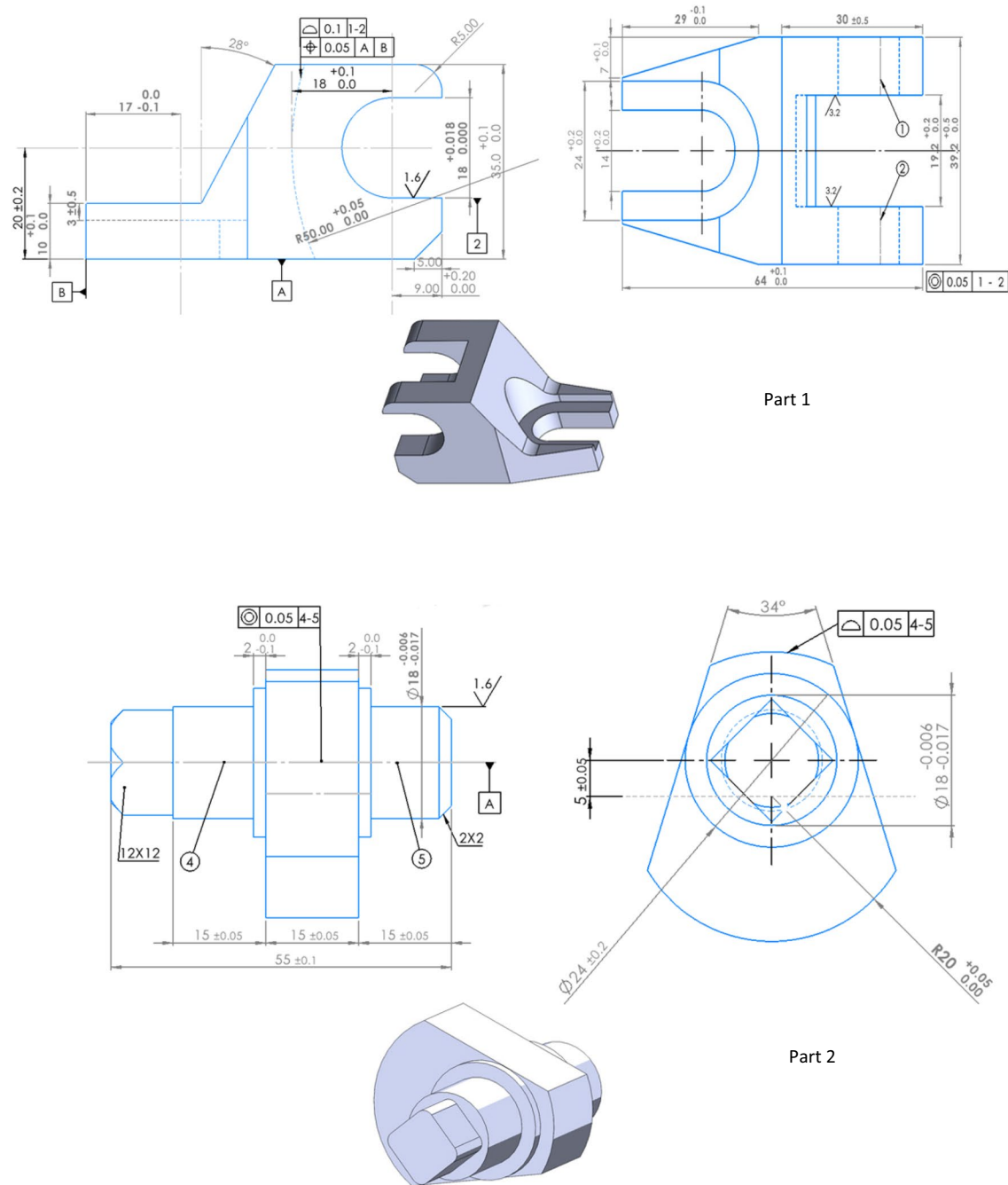


Fig. 3 Mechanical drawing and critical dimensional specifications of the cam-clamping device

5. Utilize the Jacobian–Torsor model to calculate actual Functional Requirement (FR) values.
6. Analyze FR results statistically, simultaneously quantifying the confidence interval (CI) using bootstrap-generated means.
7. Compare the calculated FR with the specified FR. If misalignment occurs, adjust tolerances based on bootstrap-generated data. Iterate until convergence with a predefined deviation limit.

The meticulous use of the bootstrap technique, assigning normal distributions to each functional element, ensures comprehensive uncertainty analysis. Subsequently, the mean undergoes the bootstrap process 10,000 times, facilitating the establishment of a confidence interval. This approach offers a robust and flexible method for uncertainty analysis, particularly valuable for dealing with complex or unknown distributions. The integrated process aligns with an iterative synthesis

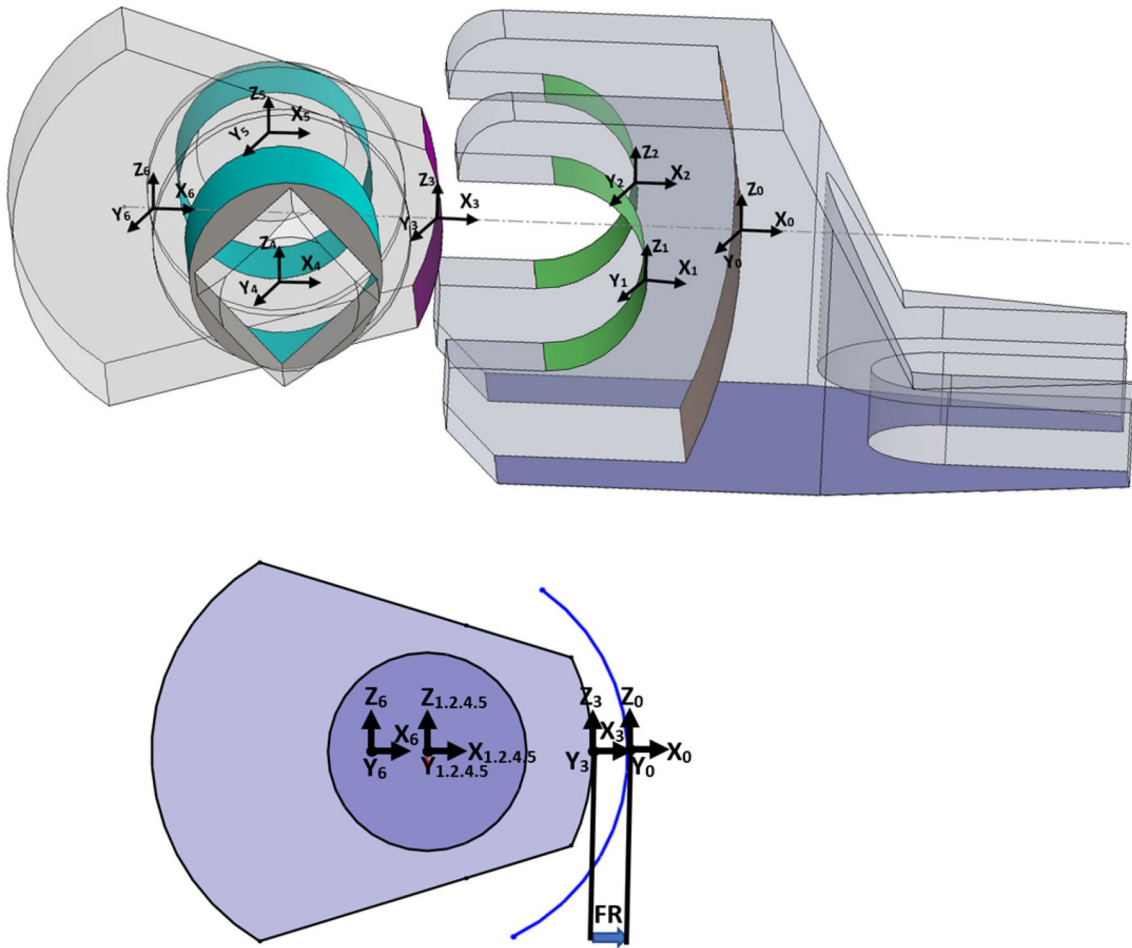


Fig. 4 Contact surfaces and FR of a mechanism

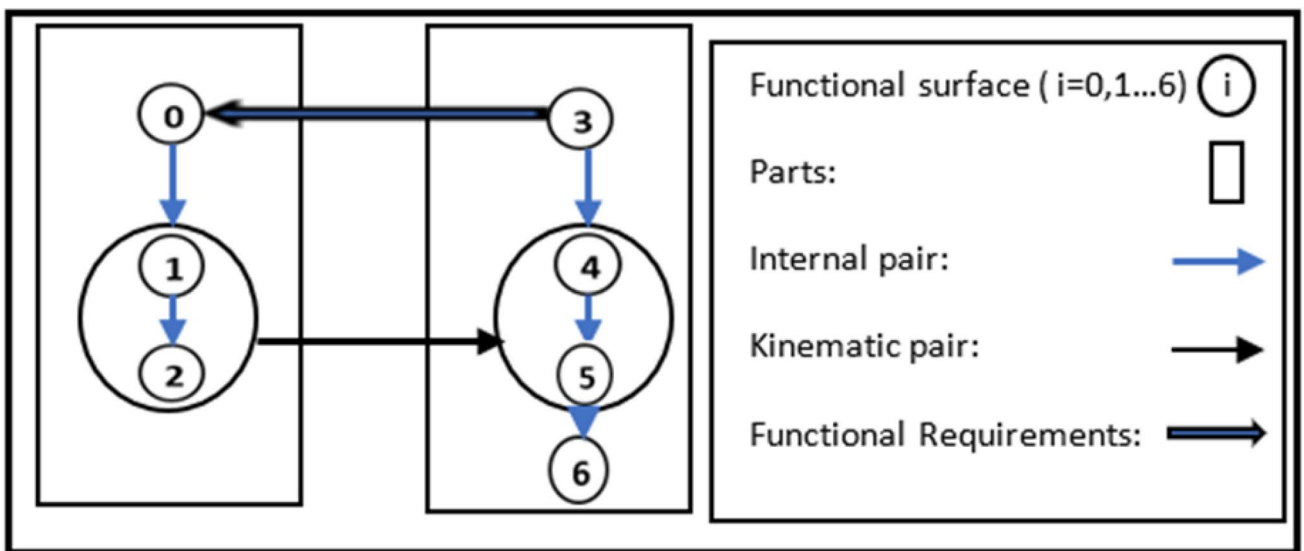


Fig. 5 Connection graph of mechanism

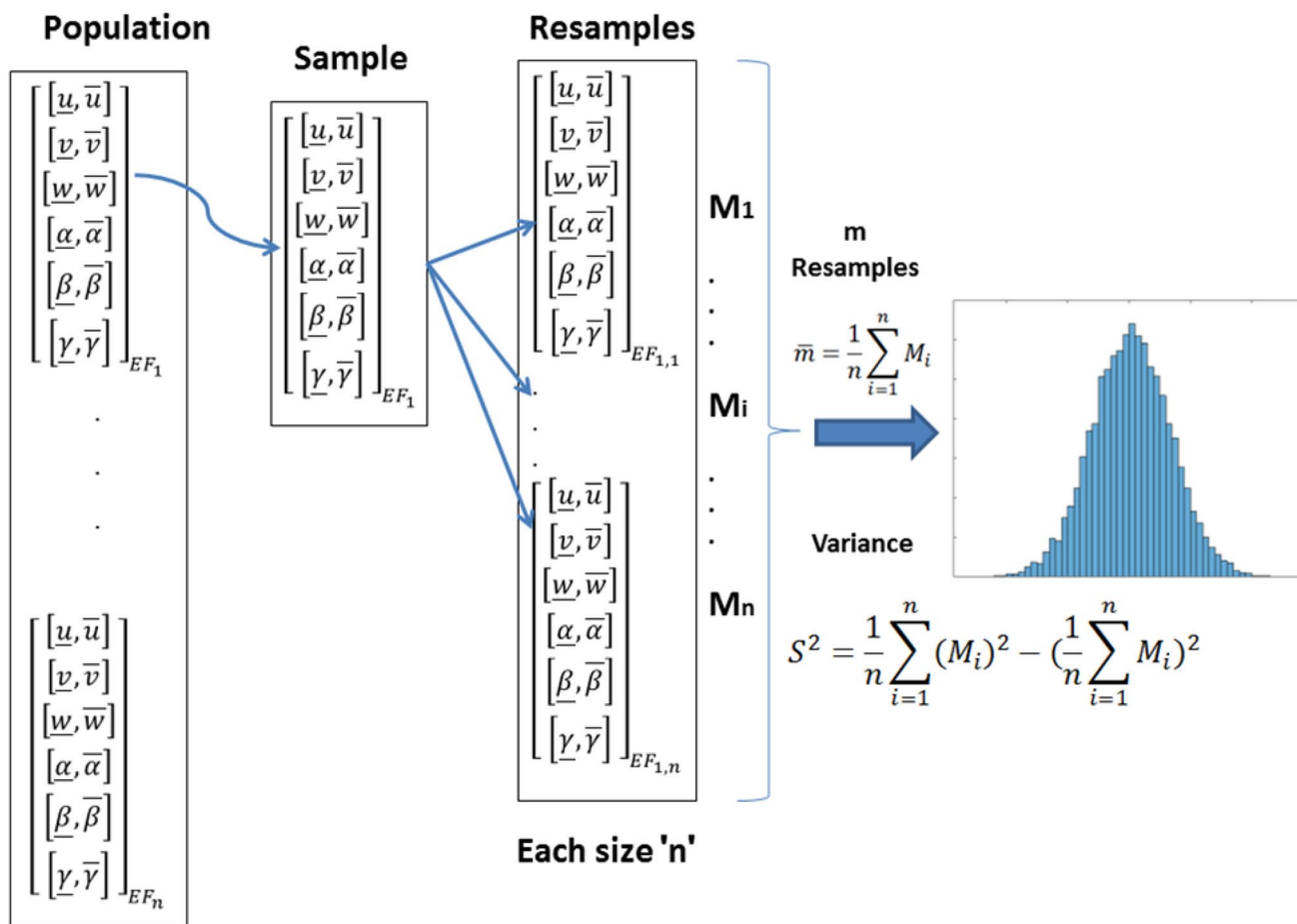


Fig. 6 Bootstrap process for SDT components

methodology, supporting engineers in selecting optimized tolerances for mechanical assemblies.

Table 3, presents a comprehensive analysis of tolerance parameters for various Functional Elements (FE) in a system. Parameters such as u_1 and u_2 exhibit symmetrical distributions within specified tolerance limits, showcasing precise and consistent values around the averages. The low standard deviation and narrow confidence intervals indicate high control and stability. Similarly, u_3 demonstrates a narrow tolerance range with a remarkably low standard deviation, emphasizing a highly controlled and consistent parameter. u_4 and u_6 have averages precisely at the midpoint of their tolerance limits, with u_4 showing stability and u_6 having a wider dispersion. u_5 , with a negative average, exhibits a well-defined and narrow confidence interval, indicating consistent deviation within specified limits. Overall, the bootstrap standard deviation and confidence intervals provide valuable insights into the precision and consistency of each parameter, highlighting effective control within their respective tolerance constraints.

The functional requirement in direction X can be calculated as

$$FR_c = 0.025 + 0.025 + 0.009 + 0 - 0.0385 + 0 = 0.0205 \tag{13}$$

According to Ghie [2009] [4], the dispersion can be calculated as

$$\delta FR_c = \sum_{i=1}^6 \frac{\sigma_i}{\sqrt{N}} = \frac{\sigma_1 + \sigma_2 + \sigma_3 + \sigma_4 + \sigma_5 + \sigma_6}{\sqrt{N}} \tag{14}$$

$$\delta FR_c = \frac{0.0015 + 0.0015 + 5.63 \times 10^{-4} + 0.0011 + 0.0014 + 0.0032}{\sqrt{10000}}$$

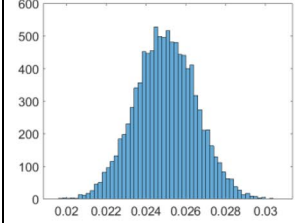
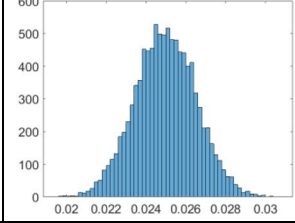
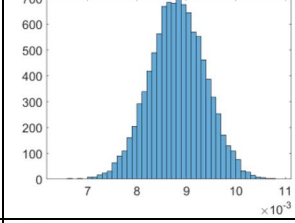
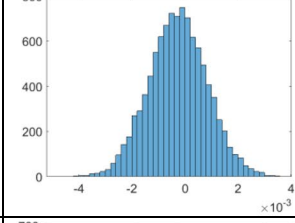
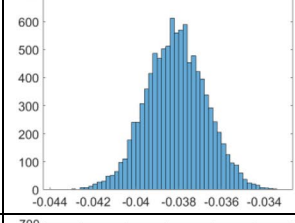
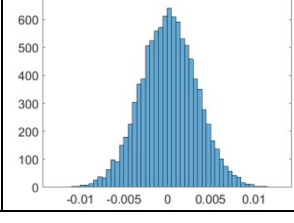
$$\delta FR_c = 9.26 \times 10^{-5}$$

The functional requirement with uncertainty (FR_u), derived through statistical analysis, is determined as:

$$FR_u = 0.0205 \pm 9.26 \times 10^{-5}$$

To enhance the reliability of this result, the mean and standard deviation of FR_u undergo a thorough bootstrap

Table 3 Summary of the bootstrap confidence interval and the bootstrap distribution for the mean of each functional element

FE	Tolerance limits	Average	Bootstrap Standard deviation	95% bootstrap confidence interval	Bootstrap distribution
u_1	[0.0, 0.05]	0.025	0.0015	[0.022, 0.028]	
u_2	[0.0, 0.05]	0.025	0.0015	[0.022, 0.028]	
u_3	[0.0, 0.018]	0.009	5.63×10^{-4}	[0.0077, 0.0099]	
u_4	[-0.0175, 0.0175]	0	0.0011	[-0.0024, 0.0019]	
u_5	[-0.006, -0.017]	-0.0385	0.0014	[-0.0409, -0.0354]	
u_6	[-0.05, 0.05]	0	0.0032	[-0.0062, 0.0065]	

process through 10,000 iterations, resulting in a comprehensive confidence interval (CI) illustrated in Fig. 7. Employing a large sample size in this statistical distribution process ensures conformance to a normal distribution, as visually

represented in the same figure. It is important to emphasize that a specified rejection rate of 5% has been consistently applied throughout these calculations.

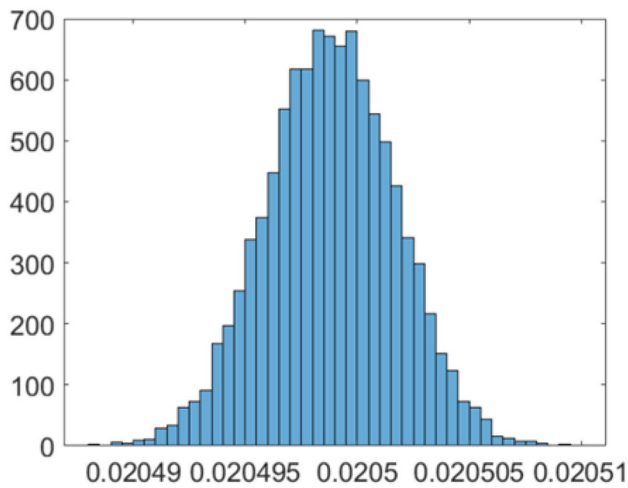


Fig. 7 Bootstrap simulation applied to functional requirement FR

The resulting confidence interval, graphically depicted in Fig. 6, showcases the range within which the true value of FR_u is likely to fall based on statistical considerations.

To evaluate the effectiveness of the chosen method, a comparative study was conducted using four techniques: bootstrap, stratified sampling, Bayesian statistics, and the analytical method. This analysis aimed to identify the most suitable approach for managing uncertainties in our data, considering not only the mean and confidence intervals but also additional statistical moments such as standard deviation and the proportion of non-conformance (P(NC)). The results are summarized in Table 4 and visually represented in Fig. 8.

Results show that, all four methods yielded nearly identical means (approximately 28.218) and confidence intervals, demonstrating a high level of consistency. The confidence intervals are also very similar, ranging from approximately 28.173 to 28.264, which indicates that each method can

Table 4 Summary of statistical analysis methods

Method	Mean	CI_Lower	CI_Upper	Std_Dev	P(NC)	Best use case
Bootstrap	28.218	28.173	28.264	8.503	0.160	Small/complex datasets, unknown distribution
Stratified sampling	28.217	28.173	28.262	8.501	0.161	Heterogeneous populations with well-defined strata
Bayesian statistics	28.218	28.174	28.262	8.504	0.160	Incorporating prior knowledge, iterative updates
Analytical method	28.218	28.174	28.262	8.500	0.160	Large datasets with known distributions

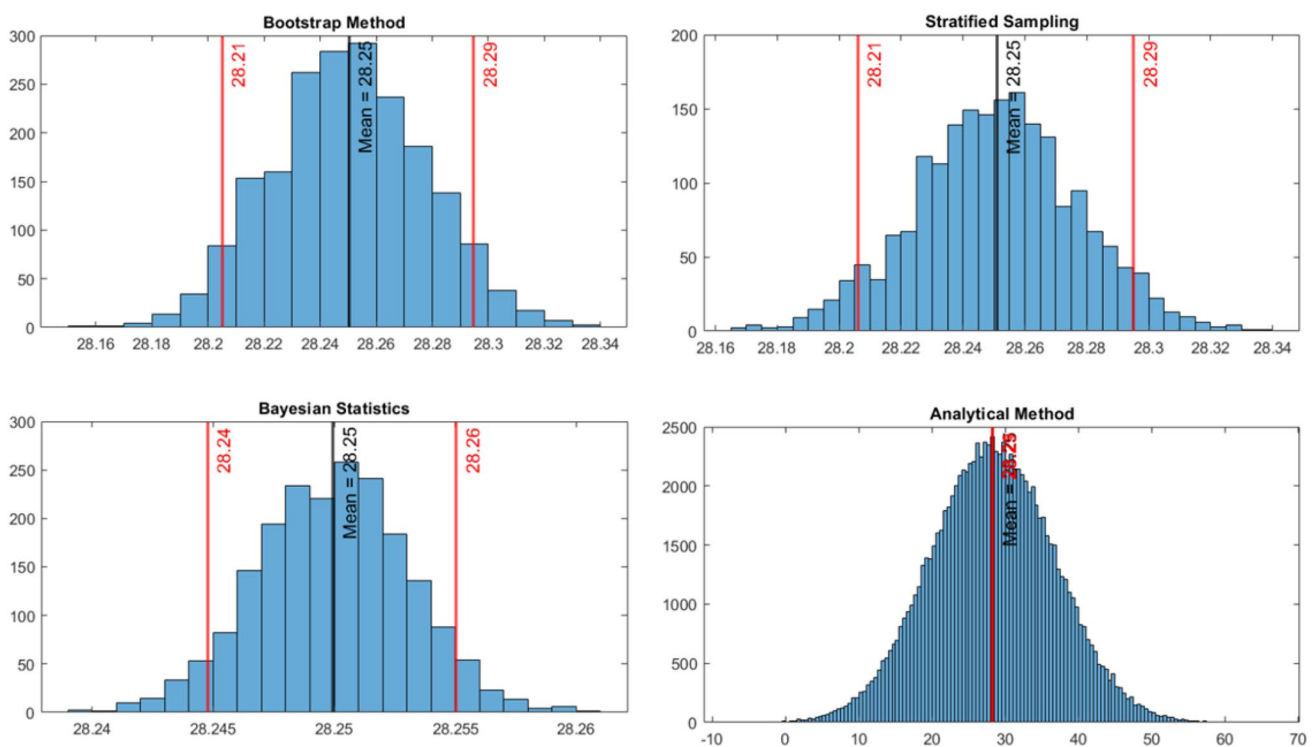


Fig. 8 Comparison of histogram distributions for different statistical analysis methods

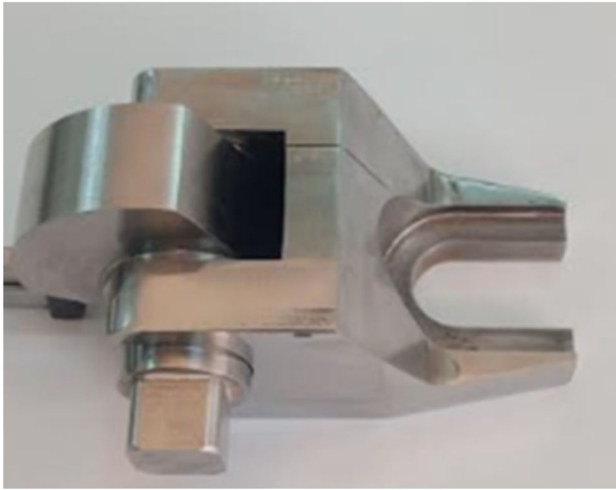


Fig. 9 Fabricated cam-clamping device

estimate the central tendency with similar precision. This consistency is clearly illustrated in Fig. 8 and Table 4.

The standard deviation (Std_Dev) is another important metric, reflecting data variability. The standard deviations for the methods are very close, around 8.5, suggesting that all methods capture the data's variability effectively. The slight variations in Std_Dev highlight how each method manages sample fluctuations, which is depicted in the figure.

The proportion of non-conformance measures the likelihood that a product fails to meet specifications. The P(NC) values are almost identical across all methods, around 0.160. This uniformity indicates that each method is equally effective in predicting defect likelihoods or deviations from desired specifications, as shown in the figure.

Each method has specific scenarios where it excels:

- Bootstrap is particularly beneficial for small or complex datasets where the underlying distribution is unknown. Its flexibility and non-parametric nature make it highly adaptable.
- Stratified sampling is optimal for heterogeneous populations with well-defined strata, ensuring appropriate representation of each subgroup and enhancing estimate precision.
- Bayesian statistics is ideal when prior knowledge is available and iterative updates are necessary, allowing for the incorporation of previous information to improve prediction accuracy.
- Analytical method is suitable for large datasets with known distributions, requiring fewer computational resources and providing quick, reliable estimates when the underlying distribution is well understood.

Despite the similar results in terms of mean, confidence intervals, standard deviation, and proportion of non-conformance across all four methods, the Bootstrap method stands out for its flexibility and suitability for small or complex datasets with unknown distributions. Its non-parametric nature and ability to handle diverse data scenarios make it a strong candidate for tolerance analysis in manufacturing processes.

Given these metrics and the specific applications for each method, the bootstrap method emerges as the most effective choice for this context. It offers both reliability and adaptability in managing the uncertainties inherent in the manufacturing of cam-clamping devices.

Conclusively, after an extensive series of calculations and analyses, the dimensions and tolerances depicted in Fig. 3 underwent a meticulous update. Subsequently, each component was precisely machined utilizing a CNC machine tool, ensuring the accurate implementation of the refined specifications. The various machined parts were systematically assembled to construct the final cam-clamping device, a culmination of the rigorous engineering and precision adjustments made during the tolerance redesign process. The resulting assembled cam-clamping device, showcased in Fig. 9, stands as a tangible embodiment of the iterative synthesis methodology applied to achieve optimal tolerances. This visual representation not only underscores the successful implementation of the refined specifications but also serves as a testament to the effectiveness of the integrated approach, harmonizing the unified Jacobian–Torsor model with Monte Carlo simulation and the bootstrap technique.

7 Conclusion

In the design phase, precise tolerance analysis is essential for ensuring that components meet geometric and dimensional constraints, thereby optimizing performance and achieving quality standards efficiently. This study introduces a novel approach to precision engineering through the integration of the unified Jacobian–Torsor model with Monte Carlo simulation and the Bootstrap technique.

A comparative evaluation of four statistical methods—bootstrap, stratified sampling, Bayesian statistics, and the analytical method—demonstrates that while all methods yield similar means, confidence intervals, and standard deviations, the bootstrap technique emerges as particularly advantageous. With nearly identical results across methods, the bootstrap technique's flexibility and non-parametric nature make it especially suited for handling small or complex datasets with unknown distributions.

The application of this integrated methodology to a cam-clamping device illustrates its practical efficacy. By refining and updating dimensions and tolerances through iterative statistical analysis, this approach not only achieves optimal tolerances but also highlights the importance of uncertainty management in precision engineering. This study advances the field of statistical tolerance redesign and provides a valuable framework for design engineers seeking to optimize tolerances in complex mechanical assemblies. The successful application in real-world scenarios attests to the approach's robustness and practical utility in manufacturing processes.

Authors' contributions The paper was a collaborative effort involving multiple contributors, each making distinct contributions. Belkacem Aoufi conducted the literature review, experiments, and analysis, and authored the paper. Hacene Ameddah and Mohamed Slamani served as project supervisors, providing the research concept, technical direction, and continuous support. They also participated in the analysis and played a role in finalizing the article. Mustapha Arslane contributed significantly to discussions and the refinement of the final draft. All authors thoroughly reviewed and approved the final manuscript for publication.

Funding This work was funded by the Ministry of Higher Education and Scientific Research of Algeria (MESRS), (grant # PRFU Project-N A11N01UN280120220003).

Data availability All data presented in this paper are available.

Code availability Can be made available upon request.

Declarations

Ethics approval Not applicable.

Consent to participate All authors contribute and participate in the work carried out in this paper.

Consent for publication The authors of this paper agree to publish this work in the International Journal of Advanced Manufacturing Technology.

Competing interests The authors declare that they have no competing interests.

References

- Chen H, Jin S, Li Z, Lai X (2014) A comprehensive study of three dimensional tolerance analysis methods. *Comput Des* 53:1–13
- Desrochers A, Ghie W, Laperriere L (2003) Application of a unified Jacobian—torsor model for tolerance analysis. *J Comput Inf Sci Eng* 3(1):2–14
- Ghie W, Laperriere L, Desrochers A (2010) Statistical tolerance analysis using the unified Jacobian-Torsor model. *Int J Prod Res* 48(15):4609–4630
- Ghie W (2009) Statistical analysis tolerance using jacobian torsor model based on uncertainty propagation method. *Int J Multiphys* 3(1):11–30. <https://doi.org/10.1260/175095409787924472>
- Song C, Zhou Y, Luo C (2019) Geometric tolerance modeling method based on B-spline parameter space envelope. *IEEE Int Conf Mechatron Autom (ICMA)* 2019:2058–2063
- Chen H, Li X, Jin S (2021) A statistical method of distinguishing and quantifying tolerances in assemblies. *Comput Ind Eng* 156:107259
- Hillyard RC, Braid IC (1978) Analysis of dimensions and tolerances in computer-aided mechanical design. *Comput Des* 10(3):161–166
- Light R, Gossard D (1982) Modification of geometric models through variational geometry. *Comput Des* 14(4):209–214
- Gaunet D (1993) Vectorial tolerancing model. *Proceedings of the 3rd CIRP Seminar on Computer-Aided Tolerancing*. Ecole Normale Supérieure de Cachan, Cachan, France. Eyrolles Press, Paris
- Ameta G, Davidson JK, Shah JJ (2018) Statistical tolerance analysis with T-Maps for assemblies. *Procedia Cirp* 75:220–225
- Desrochers A, Clément A (1994) A dimensioning and tolerancing assistance model for CAD/CAM systems. *Int J Adv Manuf Technol* 9(6):352–361. <https://doi.org/10.1007/BF01748479>
- Bernstein NS, Preiss K (1989) Representation of tolerance information in solid models. pp 37–48. <https://doi.org/10.1115/DETC1989-0018>
- Kramer GA (1992) Solving geometric constraint systems: a case study in kinematics. MIT press
- Requicha AAG (1983) Toward a theory of geometric tolerancing. *Int J Rob Res* 2(4):45–60
- Requicha AAG (1984) Representation of tolerances in solid modeling: issues and alternative approaches. In: Pickett MS, Boyse JW (eds) *Solid Modeling by Computers: From Theory to Applications*. Springer, Boston, pp 3–22
- Li H, Zhu H, Li P, He F (2014) Tolerance analysis of mechanical assemblies based on small displacement torsor and deviation propagation theories. *Int J Adv Manuf Technol* 72:89–99
- Teissandier D, Couetard Y, Gérard A (1999) A computer aided tolerancing model: proportioned assembly clearance volume. *Comput Des* 31(13):805–817
- Whitney DE, Gilbert OL, Jastrzebski M (1994) Representation of geometric variations using matrix transforms for statistical tolerance analysis in assemblies. *Res Eng Des* 6:191–210
- Fleming A (1988) Geometric relationships between toleranced features. *Artif Intell* 37(1–3):403–412
- Taguchi G (1978) Performance analysis design. *Int J Prod Res* 16(6):521–530
- Bazdar A, Kazemzadeh RB, Niaki STA (2015) Variation source identification of multistage manufacturing processes through discriminant analysis and stream of variation methodology: a case study in automotive industry. *J Eng Res* 3:1–14
- Lafond P, Laperrière L (1999) Jacobian-based modeling of dispersions affecting pre-defined functional requirements of mechanical assemblies. In: *Proceedings of the 1999 IEEE International Symposium on Assembly and Task Planning (ISATP'99)*(Cat. No. 99TH8470), pp. 20–25
- Laperrière L, ElMaraghy HA (2000) Tolerance analysis and synthesis using Jacobian transforms. *CIRP Ann* 49(1):359–362
- Cai W, Hu SJ, Yuan JX (1997) A variational method of robust fixture configuration design for 3-D workpieces. *J Manuf Sci Eng* 119(4A):593–602
- Portman VT, Weill RD (1996) Modelling spatial dimensional chains for CAD/CAM applications. In: Kimura F (ed) *Computer-aided Tolerancing*. Springer Netherlands, Dordrecht, pp 71–85
- Rivest L, Fortin C, Morel C (1993) Tolerancing a solid model with a kinematic formulation. In *Proceedings on the second ACM symposium on Solid modeling and applications*, p 357–366
- Laperrière L, Lafond P (1999) Modeling tolerances and dispersions of mechanical assemblies using virtual joints. *Int Des Eng Tech Conf Comput Inf Eng Conf* 19715:933–942

28. Yi Y et al (2024) A novel assembly tolerance analysis method considering form errors and partial parallel connections. *Int J Adv Manuf Technol* 131(11):5489–5510
29. Peng H, Peng Z (2020) An iterative method of statistical tolerancing based on the unified Jacobian-Torsor model and Monte Carlo simulation. *J Comput Des Eng* 7(2):165–176
30. Roth M, Schleich B, Wartzack S (2022) Handling sampling-induced uncertainties in tolerance-cost optimization. *Procedia CIRP* 114:209–214
31. Ding S, Zheng X, Bao J, Zhang J (2021) An improved Jacobian-Torsor model for statistical variation solution in aero-engine rotors assembly. *Proc Inst Mech Eng Part B J Eng Manuf* 235(3):466–483
32. Liu T, Cao Y-L, Zhao Q, Yang J, Cui L (2019) Assembly tolerance analysis based on the Jacobian model and skin model shapes. *Assem Autom* 39(2):245–253
33. Wang H et al (2015) Integrated analysis method of thin-walled turbine blade precise machining. *Int J Precis Eng Manuf* 16:1011–1019
34. Zhang C, Ben Wang H-P (1993) Tolerance analysis and synthesis for cam mechanisms. *Int J Prod Res* 31(5):1229–1245
35. Chang W-T, Wu L-I (2013) Tolerance analysis and synthesis of cam-modulated linkages. *Math Comput Model* 57(3–4):641–660
36. Rothbart HA, Klipp DL (2004) *Cam design handbook*. *J Mech Des* 126(2):375
37. Norton RL (2002) *Cam design and manufacturing handbook*. Industrial Press Inc
38. Norton RL (1988) Effect of manufacturing method on dynamic performance of cams—An experimental study. part I—eccentric cams. *Mech Mach Theory* 23(3):191–199
39. Chase KW, Parkinson AR (1991) A survey of research in the application of tolerance analysis to the design of mechanical assemblies. *Res Eng Des* 3(1):23–37
40. Creveling CM (1997) Book review: tolerance design: a handbook for developing optimal specifications. *I&CS Instrum Control Syst* 70(2):10
41. Zhang C, Ben Wang HP (1993) Tolerance analysis and synthesis for cam mechanisms. *Int J Prod Res* 31(5):1229–1245. <https://doi.org/10.1080/00207549308956785>
42. Molloy O, Warman EA, Tilley S (2012) *Design for Manufacturing and Assembly: Concepts, architectures and implementation*. Springer Science & Business Media
43. Boothroyd G, Dewhurst P, Knight WA (2010) *Product design for manufacture and assembly*. CRC Press
44. Khodaygan S, Movahhedy MR, SaadatFomani M (2010) Tolerance analysis of mechanical assemblies based on modal interval and small degrees of freedom (MI-SDOF) concepts. *Int J Adv Manuf Technol* 50:1041–1061
45. Ghie W (2009) Statistical analysis tolerance using jacobian torsor model based on uncertainty propagation method. *Int J Multiphys* 3(1):11–30
46. Tsai L-W (1999) *Robot analysis: the mechanics of serial and parallel manipulators*. John Wiley & Sons
47. Hervé JM (1978) Analyse structurelle des mécanismes par groupe des déplacements. *Mech Mach Theory* 13(4):437–450
48. Rab S et al (2019) Comparison of Monte Carlo simulation, least square fitting and calibration factor methods for the evaluation of measurement uncertainty using direct pressure indicating devices. *Mapan* 34:305–315
49. Kirkup L, Frenkel RB (2006) *An introduction to uncertainty in measurement: using the GUM (guide to the expression of uncertainty in measurement)*. Cambridge University Press
50. Elster C (2014) Bayesian uncertainty analysis compared with the application of the GUM and its supplements. *Metrologia* 51(4):S159
51. Efron B, Tibshirani RJ (1994) *An introduction to the bootstrap*. CRC Press

Publisher's Note Springer Nature remains neutral with regard to jurisdictional claims in published maps and institutional affiliations.

Springer Nature or its licensor (e.g. a society or other partner) holds exclusive rights to this article under a publishing agreement with the author(s) or other rightsholder(s); author self-archiving of the accepted manuscript version of this article is solely governed by the terms of such publishing agreement and applicable law.